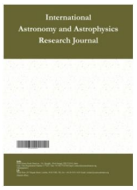

International Astronomy and Astrophysics Research Journal

3(1): 86-100, 2021; Article no.IAARJ.70329

Singly Ionized Iridium Spectral Lines in the Atmosphere of Hot Stars

Zoran Simić[1*], Nenad M. Sakan[2], Nenad Milovanović[1] and Mihailo Martinović[3,4]

[1] *Astronomical Observatory, Volgina 7, 11060 Belgrade, Serbia.*
[2] *University of Belgrade, Institute of Physics, P.O.Box 57, 11001 Belgrade, Serbia.*
[3] *Lunar and Planetary Laboratory, University of Arizona, Tucson, AZ 85721, USA.*
[4] *LESIA, Observatoire de Paris, Meudon, France.*

Authors' contributions

This work was carried out in collaboration among all authors. All authors read and approved the final manuscript.

Article Information

Editor(s):
(1) Prof. Magdy Rabie Soliman Sanad, National Research Institute of Astronomy and Geophysics, Egypt.
(2) Prof. Hadia Hassan Selim, National Research Institute of Astronomy and Geophysics, Egypt.
Reviewers:
(1) Feyisso Sado Bedecha, Addis Ababa University, Jigjiga University, Ethiopia.
(2) Rahul Singh, India.
(3) Ricardo Gobato, Secretariat of State of Parana Education and Sport (SEED/PR), Laboratory of Biophysics and Molecular Modeling Genesis, Brazil.
(4) Gemechu Muleta Kumssa, Ethiopian Space Science and Technology Institute (ESSTI), Ethiopia.
(5) Dmitry Tsipenyuk, Moscow Polytechnic University, Russia.
Complete Peer review History: http://www.sdiarticle4.com/review-history/70329

Original Research Article

Received 09 May 2021
Accepted 14 July 2021
Published 19 July 2021

ABSTRACT

The electron-impact broadening parameters of ion lines are of interest for a number of problems in astrophysical, laboratory, and technological plasma investigations. Singly ionized Iridium lines are confirmed their presence in stellar spectra of the chemically peculiar stars. Our calculations are performed using the modified semiempirical method of Dimitrijević and Konjević. Stark widths for 301 Ir II spectral lines are presented. From the calculated list of lines, the 21 strongest lines from the iridium spectrum are selected with high value of intensity $\geq$ 3000 to demonstrate importance of the Stark broadening mechanism for different types of stars. The analysis of the electron-impact effect on spectral line shapes are performed and obtained Stark and Doppler withds are compared.

**Corresponding author: E-mail: zsimic@aob.rs;*

Keywords: Atomic data; lines; plasmas.

2010 Mathematics Subject Classification: 53C25; 83C05; 57N16.

1 INTRODUCTION

The chemically peculiar (CP) stars of the upper main sequence, usually it has been classified as Bp, Ap, HgMn, or Am type of stars. Spectroscopy of these CP stars plays important role for resolving the elemental abundances and physical processes in their atmospheres. Today's satellite spectroscopy provides high-resolution spectra, making heavy elements very important and available for research in astrophysics. In [1] it is noted Goddard High Resolution Spectrograph (GHRS) on board the Hubble Space Telescope at an average resolution of 0.023 Å. GHRS observations of χ Lupi have become a useful source of data for atomic spectroscopy, displaying many transitions that are difficult to observe in a laboratory setting. This project has been successful in determining abundances for more than 50 elements. In [2] it is reported 4d-elements and 5d-elements in CP stars of Hg-Mn type and the interpretation of their spectra II and III.

Quantitatively accurate analysis and theoretical interpretation of the spectrum of CP stars requires available atomic data, wavelengths, transition probabilities, hyperfine structure and isotopic shifts for the lowest ionization states of many elements. The abundance of an element is a key parameter in the observability of spectral lines. Significance of these data for heavy and rare-earth elements (REE) in stellar spectra is increasing, as noted in [3, 4] where one can see that the REE are overabundant in CP stars. As atomic number increases, the cosmic abundance drops. Usually, as spectroscopic abundances from the solar photosphere become more reliable, they tend to confirm the meteoritic values [5, 6]. Chemical composition data for the Sun can be derived from very different layers, from the center to the outermost coronal layers.

Electron configuration of Iridium follows noble xenon gas [Xe] $4f^{1}45d^{7}6s^{2}$. Iridium has two stable isotopes $^{1}91$Ir and $^{1}93$Ir with abundances of 37.3% and 62.7% and nuclear spins 3/2 [7].

The determination of abundance for osmium and iridium for χ Lupi star has followed the techniques used in previous analyses performed in [8]. Since the observed spectrum is a combination of spectra from both stars of the binary system, a synthetic spectrum was generated for each star for short wavelength intervals that included each of the spectral lines studied.

In [9], it is presented experimentally determined wavelengths and oscillator strengths for 27 Os II and 23 Ir II transitions. The oscillator strengths have been determined by combining radiative lifetimes measured using the laser-induced fluorescence technique with branching fractions determined from Fourier transform spectrometer emission line intensities. This new data were used in a synthetic spectrum analysis of high-resolution ultraviolet spectra of χ Lupi obtained with the Hubble Space Telescope. Weak abundance enhancements were determined for both elements, [Os/H] = +1.3 dex and [Ir/H] = +0.7 dex. In the case of iridium only one reasonably unblended line of Ir II was identified in stellar spectra [9]. Its analysis followed a similar method as for the lines of Os II. The fit to the line Ir II λ=2152.706 Å is presented in their work, with the best fit abundance value of (Ir/H)= log(ϵ_{Ir}) - log(ϵ_{H}) = 2.05, on a scale where log(ϵ_{H})=12, representing an abundance enhancement of +0.7 dex with respect to the solar system.

Mentioned article was the main motivation for our work on iridium spectral lines. The presence of these lines in stellar plasma emphasized the need to know the parameters for Stark broadening. The atomic data of such rare elements have only become available recently. Our contribution is an effort to combine mentioned stellar processes with the pointing out a need for the experimental data and, as such, to open a path for more sophisticated spectroscopy with the help of the estimated Stark parameters.

The spectrum of Ir II has been measured in the wavelength region of approximately 1250 Å to 4750 Å. The ground level system is associated

with the electron configurations $5d^8$, $5d^7 6s$ and $5d^6 6s^2$, which are strongly mixed [10]. In this system 35 levels out of 81 were identified. The energy levels have been adjusted by least-squares level optimization using the LOPT code [11].

2 THEORETICAL METHOD

Theoretical method for calculations which is used here for Stark widths of Ir II spectral lines is based on the modified semiempirical method (MSE) [12], valid for the Stark broadening of isolated, non-hydrogenic ion lines. Here, we note more complex semi-empirical method [13] or the semi-classical perturbation method [14, 15]. In comparison with these methods MSE needs less atomic data. Therefore, it is more applicable in the case of more complex spectra of heavier elements such as iridium. Due to a very complex spectrum of Ir II it was not possible to adequately use the MSE approach, so we used the simplified version of this approach given in [16]

For all 301 calculated lines we used the energy levels obtained from NIST ADS databases [10, 11]. The matrix elements needed for the present calculations are obtained within the Coulomb approximation formalism [17], while the line and multiplet factors are taken from [18] whenever it is necessary.

In the case when more sophisticated methods are not applicable we can use approximate formula [19] which is simple and sometimes very useful in astrophysics, especially when data for a large number spectral lines are needed, and they are missing in existing literature and databases.

The accuracy of the MSE approximation used in the calculation of Stark broadening parameters is assumed to be about 50%. In the case of the emitters with very complex spectra (e.g., Xe II and Kr II) MSE approach gives a very good agreement with experimental measurements (in the interval 30%), see [20, 21].

3 RESULTS

The calculations of Stark widths (FWHM) for electron-impact broadening, have been performed for a perturber density of 10^{17} cm^{-3} and for a temperature value of 10000K, see Table 1. The order of transitions in our table follows the list of spectral lines from the NIST database, which made it easier to monitor and observe atomic data for spectroscopy. The transformation of Stark width in Å to the width expressed in angular frequency units may be performed using the following formula, see [3, 4]:

$$W(\mathring{A}) = \frac{\lambda^2}{2\pi c} W(s^{-1}) \tag{3.1}$$

where c is the speed of light. For synthetic spectrum calculations it is more convenient to use following expression for the different temperatures:

$$W(s^{-1}) = A_0 T^{-1/2} \tag{3.2}$$

where A_0 represent constant determined with the best fit, for detailes about this and following equation refered to [22]. In our Table 1. for all 301 spectral lines of iridium it is presented by columns: transition between levels, wavelength in Å, Full Width at Half Maximum in Å, and logarithmic form for Stark width per electron and temperature of 10000K noted with log W.

For A-type stars the most representiv value for temperature is 10000K where the Stark broadening becomes the dominant pressure broadening mechanism due to hydrogen ionization. In many cases there is a good approximation with next expression.

$$W_o = (T/T_o)^{-1/2} W_{T_o} \tag{3.3}$$

where W_{T_o} represent Stark width at T_o=10000K. With this we can obtained Stark width at any value of temperatures from 10 000 K to 300 000 K.

Table 1. Calculated parameters for Ir II spectral lines

Transition	λ(Å)	FWHM(Å)	logW
5d^8 ^{3}F$_4$ - 6548$^o_3$	1581.8	0.0076	-6.241
5d^7(^{4}F)6s ^{5}F$_5$ - 6273$^o_4$	1594.0	0.0268	-5.702
5d^8 ^{3}P$_2$ - 6580$^o_2$	1594.5	0.0080	-6.226
5d^8 ^{3}P$_2$ - 6548$^o_3$	1602.8	0.0078	-6.242
5d^7(^{4}F)6s ^{5}F$_4$ - 6690$^o_3$	1609.8	0.0317	-5.638
5d^7(^{4}F)6s ^{5}F$_5$ - 6197$^o_5$	1613.7	0.0269	-5.711
5d^8 ^{3}P$_2$ - 6420$^o_3$	1636.2	0.0070	-6.307
5d^7(^{4}F)6s ^{5}F$_4$ - 6548$^o_3$	1647.6	0.0318	-5.656
5d^8 ^{3}P$_2$ - 6376$^o_2$	1648.1	0.0067	-6.332
5d^8 ^{3}F$_4$ - 6273$^o_4$	1653.7	0.0059	-6.391
5d^8 ^{3}F$_4$ - 6197$^o_5$	1674.8	0.0054	-6.440
5d^8 ^{3}F$_4$ - 6148$^o_4$	1688.4	0.0051	-6.473
5d^8 ^{1}D$_2$ - 6690$^o_3$	1726.1	0.0105	-6.177
5d^7(^{4}F)6s ^{5}F$_3$ - 6580$^o_2$	1735.6	0.0363	-5.644
5d^8 ^{3}P$_2$ - 5d^7(^{4}F$_{9/2}$)6p (9/2,3/2)$^o_3$	1747.5	0.0044	-6.563
5d^7(^{4}F)6s ^{5}F$_4$ - 6197$^o_5$	1748.8	0.0324	-5.700
5d^8 ^{3}P$_1$ - 6580$^o_2$	1762.3	0.0097	-6.228
5d^8 ^{1}D$_2$ - 6548$^o_3$	1769.7	0.0095	-6.244
5d^7(^{4}F)6s ^{5}F$_3$ - 6454$^o_3$	1774.5	0.0366	-5.660
5d^7(^{4}F)6s ^{5}F$_5$ - 5d^7(^{4}F$_{9/2}$)6p (9/2,3/2)$^o_4$	1778.3	0.0279	-5.779
5d^8 ^{3}P$_2$ - 5d^7(^{4}P$_{3/2}$)6p (3/2,1/2)$^o_2$	1784.3	0.0036	-6.669
5d^8 ^{1}G$_4$ - 7311$^o_4$	1788.9	0.0199	-5.931
5d^7(^{4}F)6s ^{3}F$_4$ - 6678$^o_5$	1816.0	0.0417	-5.623
5d^8 ^{3}F$_3$ - 6454$^o_3$	1831.1	0.0091	-6.293
5d^7(^{4}F)6s ^{5}F$_2$ - 6580$^o_2$	1834.9	0.0413	-5.636
5d^8 ^{3}F$_3$ - 6420$^o_3$	1842.3	0.0088	-6.311
5d^8 ^{3}P$_0$ - 6520$^o_1$	1852.2	0.0100	-6.259
5d^8 ^{3}F$_4$ - 5d^7(^{4}F$_{9/2}$)6p (9/2,3/2)$^o_4$	1852.8	0.0015	-7.090
5d^7(^{4}F)6s ^{5}F$_1$ - 6580$^o_2$	1857.1	0.0425	-5.635
5d^8 ^{3}F$_3$ - 6376$^o_2$	1857.4	0.0085	-6.335
5d^{6}6s^2 ^{5}D$_4$ - 7311$^o_4$	1857.7	0.0551	-5.521
5d^7(^{4}F)6s ^{5}F$_5$ - 5d^7(^{4}F$_{9/2}$)6p (9/2,3/2)$^o_5$	1862.5	0.0287	-5.808
5d^7(^{4}F)6s ^{5}F$_5$ - 5d^7(^{4}F$_{7/2}$)6p (7/2,1/2)$^o_4$	1868.3	0.0287	-5.809
5d^7(^{4}F)6s ^{3}F$_4$ - 6516$^o_5$	1870.9	0.0423	-5.643
5d^7(^{4}F)6s ^{5}F$_3$ - 6148$^o_4$	1876.1	0.0376	-5.697
5d^7(^{4}F)6s ^{5}F$_1$ - 6520$^o_1$	1878.1	0.0427	-5.642
5d^7(^{4}F)6s ^{5}F$_2$ - 6454$^o_3$	1878.5	0.0418	-5.652
5d^7(^{4}P)6s ^{5}P$_3$ - 6580$^o_2$	1883.6	0.0439	-5.633
5d^7(^{4}F)6s ^{5}F$_2$ - 6420$^o_3$	1890.3	0.0419	-5.656
5d^7(^{4}F)6s ^{5}F$_2$ - 6376$^o_2$	1906.3	0.0421	-5.661
5d^7(^{4}F)6s ^{5}F$_5$ - 5d^{6}6s(^{6}D$_{9/2}$)6p (9/2,1/2)$^o_5$	1948.1	0.0296	-5.833
5d^7(^{4}P)6s ^{5}P$_3$ - 6376$^o_2$	1958.8	0.0449	-5.657
5d^8 ^{3}P$_2$ - 5d^7(^{4}F$_{3/2}$)6p (3/2,1/2)$^o_2$	1976.7	0.0330	-5.798
5d^8 ^{3}F$_3$ - 6046$^o_2$	1978.9	0.0058	-6.557
5d^7(^{4}F)6s ^{5}F$_5$ - 5d^{6}6s(^{6}D$_{9/2}$)6p (9/2,1/2)$^o_4$	1988.0	0.0301	-5.843

Table 1. Continued

Transition	λ(Å)	FWHM(Å)	logW
5d^7(^{4}F)6s ^{3}F$_4$ - 6197$^o_5$	1990.0	0.0438	-5.681
5d^7(^{4}F)6s ^{5}F$_2$ - 6147$^o_3$	1993.4	0.0433	-5.688
5d^8 ^{1}D$_2$ - 5d^7(^{4}P$_{3/2}$)6p (3/2,1/2)$^o_2$	1993.7	0.0044	-6.677
5d^7(^{4}P)6s ^{5}P$_2$ - 6580$^o_2$	1994.9	0.0502	-5.625
5d^8 ^{3}P$_2$ - 5d^7(^{4}P$_{5/2}$)6p (5/2,1/2)$^o_3$	1995.8	0.0332	-5.804
5d^8 ^{3}P$_1$ - 5d^7(^{4}P$_{3/2}$)6p (3/2,1/2)$^o_2$	1997.2	0.0045	-6.677
5d^7(^{2}G)6s ^{3}G$_3$ - 7311$^o_4$	2002.7	0.0656	-5.512
5d^7(^{4}P)6s ^{5}P$_2$ - 6548$^o_3$	2007.2	0.0503	-5.628
5d^7(^{4}F)6s ^{3}F$_4$ - 6148$^o_4$	2008.6	0.0441	-5.687
5d^8 ^{1}G$_4$ - 6690$^o_3$	2011.5	0.0143	-6.176
5d^8 ^{1}G$_4$ - 6678$^o_5$	2016.5	0.0142	-6.181
5d^7(^{4}P)6s ^{5}P$_2$ - 6520$^o_1$	2018.5	0.0505	-5.632
5d^8 ^{3}F$_2$ - 6690$^o_3$	2019.7	0.0145	-6.175
5d^8 ^{3}P$_2$ - 5d^7(^{4}F$_{5/2}$)6p (5/2,1/2)$^o_2$	2022.8	0.0336	-5.811
5d^7(^{4}F)6s ^{3}F$_3$ - 6690$^o_3$	2023.2	0.0538	-5.606
5d^{6}6s^2 ^{5}D$_3$ - 7311$^o_4$	2024.3	0.0672	-5.510
5d^8 ^{1}D$_2$ - 5d^{6}6s(^{6}D$_{3/2}$)6p (3/2,1/2)$^o_1$	2027.3	0.0037	-6.770
5d^7(^{2}G)6s ^{3}G$_5$ - 6678$^o_5$	2027.5	0.0539	-5.608
5d^7(^{4}F)6s ^{5}F$_4$ - 5d^{6}6s(^{6}D$_{7/2}$)6p (7/2,1/2)$^o_3$	2028.7	0.0355	-5.789
5d^8 ^{3}F$_3$ - 5d^7(^{4}P$_{3/2}$)6p (3/2,1/2)$^o_2$	2031.7	0.0046	-6.677
5d^8 ^{3}P$_0$ - 5d^7(^{4}P$_{1/2}$)6p (1/2,1/2)$^o_1$	2033.5	0.0060	-6.565
5d^7(^{4}F)6s ^{5}F$_2$ - 6046$^o_2$	2033.8	0.0439	-5.700
5d^8 ^{3}F$_4$ - 5d^{6}6s(^{6}D$_{9/2}$)6p (9/2,1/2)$^o_5$	2037.2	0.0329	-5.826
5d^7(^{2}G)6s ^{3}G$_5$ - 6654$^o_6$	2037.4	0.0540	-5.611
5d^7(^{4}F)6s ^{5}F$_4$ - 5d^7(^{4}F$_{9/2}$)6p (9/2,3/2)$^o_5$	2044.2	0.0357	-5.793
5d^8 ^{3}P$_2$ - 5d^7(^{4}F$_{3/2}$)6p (3/2,1/2)$^o_1$	2044.8	0.0339	-5.816
5d^7(^{4}P)6s ^{5}P$_3$ - 6148$^o_4$	2049.6	0.0462	-5.684
5d^7(^{4}P)6s ^{5}P$_3$ - 6147$^o_3$	2050.2	0.0462	-5.684
5d^7(^{4}F)6s ^{5}F$_4$ - 5d^7(^{4}F$_{7/2}$)6p (7/2,1/2)$^o_4$	2051.2	0.0358	-5.795
5d^7(^{4}F)6s ^{3}F$_4$ - 5d^7(^{4}F$_{9/2}$)6p (9/2,3/2)$^o_3$	2057.2	0.0448	-5.700
5d^7(^{4}F)6s ^{5}F$_1$ - 5d^{6}6s(^{6}D$_{1/2}$)6p (1/2,1/2)$^o_0$	2058.9	0.0452	-5.697
5d^7(^{4}F)6s ^{5}F$_3$ - 5664$^o_2$	2063.0	0.0401	-5.751
5d^7(^{4}F)6s ^{5}F$_1$ - 5d^7(^{4}P$_{1/2}$)6p (1/2,1/2)$^o_1$	2064.8	0.0453	-5.699
5d^7(^{4}F)6s ^{5}F$_4$ - 5d^7(^{4}P$_{5/2}$)6p (5/2,1/2)$^o_3$	2065.1	0.0360	-5.798
5d^8 ^{3}F$_2$ - 6580$^o_2$	2065.8	0.0134	-6.227
5d^7(^{4}F)6s ^{3}F$_3$ - 6580$^o_2$	2069.5	0.0546	-5.619
5d^8 ^{3}P$_2$ - 5d^7(^{4}P$_{5/2}$)6p (5/2,1/2)$^o_2$	2070.5	0.0342	-5.823
5d^8 ^{1}G$_4$ - 6548$^o_3$	2070.9	0.0130	-6.243
5d^7(^{4}F)6s ^{5}F$_3$ - 5d^{6}6s(^{6}D$_{5/2}$)6p (5/2,1/2)$^o_2$	2075.4	0.0403	-5.754
5d^8 ^{3}P$_2$ - 5d^7(^{4}F$_{7/2}$)6p (7/2,1/2)$^o_3$	2076.8	0.0343	-5.824
5d^7(^{2}H)6s ^{3}H$_5$ - 7311$^o_4$	2078.4	0.0714	-5.507
5d^7(^{4}P)6s ^{5}P$_2$ - 6376$^o_2$	2078.8	0.0515	-5.649
5d^8 ^{3}F$_2$ - 6548$^o_3$	2079.7	0.0131	-6.243
5d^7(^{4}F)6s ^{5}F$_3$ - 5d^7(^{4}F$_{9/2}$)6p (9/2,3/2)$^o_4$	2080.6	0.0403	-5.755
5d^8 ^{3}F$_4$ - 5d^{6}6s(^{6}D$_{9/2}$)6p (9/2,1/2)$^o_4$	2081.0	0.0335	-5.836
5d^7(^{4}F)6s ^{3}F$_3$ - 6548$^o_3$	2083.4	0.0549	-5.623

Table 1. Continued

Transition	λ(Å)	FWHM(Å)	logW
$5d^7(^4P)6s\ ^3P_2$ - 6690^o_3	2084.2	0.0577	-5.602
$5d^8\ ^1G_4$ - 6516^o_5	2084.5	0.0127	-6.259
$5d^7(^4F)6s\ ^5F_2$ - $5d^7(^4P_{3/2})6p$ (3/2,1/2)$^o_2$	2090.3	0.0448	-5.714
$5d^8\ ^3P_1$ - $5d^7(^4P_{1/2})6p$ (1/2,1/2)$^o_0$	2090.8	0.0024	-6.979
$5d^8\ ^3F_2$ - 6520^o_1	2091.9	0.0129	-6.257
$5d^7(^4P)6s\ ^5P_3$ - 6046^o_2	2093.8	0.0469	-5.695
$5d^7(^2G)6s\ ^3G_5$ - 6516^o_5	2096.2	0.0551	-5.627
$5d^8\ ^1D_2$ - 5664^o_2	2097.1	0.0022	-7.023
$5d^7(^4F)6s\ ^5F_3$ - $5d^7(^4F_{5/2})6p$ (5/2,1/2)$^o_3$	2097.3	0.0406	-5.760
$5d^66s^2\ ^5D_4$ - 6690^o_3	2098.8	0.0586	-5.601
$5d^7(^4P)6s\ ^5P_3$ - $5d^7(^4F_{9/2})6p$ (9/2,3/2)$^o_3$	2100.2	0.0471	-5.697
$5d^8\ ^3P_1$ - 5664^o_2	2101.0	0.0022	-7.023
$5d^66s^2\ ^5D_4$ - 6678^o_5	2104.3	0.0587	-5.602
$5d^8\ ^1D_2$ - $5d^66s(^6D_{5/2})6p$ (5/2,1/2)$^o_2$	2110.0	0.0019	-7.086
$5d^8\ ^1G_4$ - 6454^o_3	2112.2	0.0121	-6.291
$5d^8\ ^3P_1$ - $5d^66s(^6D_{5/2})6p$ (5/2,1/2)$^o_2$	2113.9	0.0019	-7.086
$5d^8\ ^1D_2$ - $5d^7(^4P_{3/2})6p$ (3/2,1/2)$^o_1$	2115.0	0.0018	-7.112
$5d^8\ ^3P_1$ - $5d^7(^4P_{3/2})6p$ (3/2,1/2)$^o_1$	2118.9	0.0018	-7.112
$5d^7(^4F)6s\ ^5F_1$ - $5d^7(^4P_{3/2})6p$ (3/2,1/2)$^o_2$	2119.1	0.0462	-5.712
$5d^8\ ^3F_2$ - 6454^o_3	2121.3	0.0122	-6.291
$5d^8\ ^3P_0$ - $5d^66s(^6D_{3/2})6p$ (3/2,1/2)$^o_1$	2123.6	0.0041	-6.771
$5d^7(^4F)6s\ ^3F_3$ - 6454^o_3	2125.1	0.0556	-5.634
$5d^7(^4F)6s\ ^5F_5$ - $5d^7(^4F_{9/2})6p$ (9/2,1/2)$^o_5$	2126.8	0.0319	-5.877
$5d^8\ ^1G_4$ - 6420^o_3	2127.1	0.0118	-6.309
$5d^7(^4F)6s\ ^5F_2$ - $5d^66s(^6D_{3/2})6p$ (3/2,1/2)$^o_1$	2127.9	0.0454	-5.724
$5d^8\ ^1D_2$ - $5d^7(^4F_{5/2})6p$ (5/2,1/2)$^o_3$	2132.5	0.0015	-7.218
$5d^7(^2D2)6s\ ^3D_3$ - 7311^o_4	2139.8	0.0764	-5.503
$5d^8\ ^3F_3$ - 5664^o_2	2139.9	0.0023	-7.024
$5d^7(^2G)6s\ ^3G_4$ - 6690^o_3	2144.6	0.0616	-5.598
$5d^7(^4F)6s\ ^5F_4$ - $5d^66s(^6D_{9/2})6p$ (9/2,1/2)$^o_5$	2147.8	0.0373	-5.817
$5d^7(^4P)6s\ ^3P_2$ - 6548^o_3	2148.2	0.0589	-5.619
$5d^7(^4P)6s\ ^5P_1$ - 6520^o_1	2148.7	0.0584	-5.623
$5d^7(^4F)6s\ ^5F_4$ - $5d^7(^4F_{7/2})6p$ (7/2,1/2)$^o_3$	2152.7	0.0374	-5.819
$5d^8\ ^3F_2$ - 6376^o_2	2156.7	0.0115	-6.333
$5d^7(^4F)6s\ ^3F_3$ - 6376^o_2	2160.7	0.0563	-5.643
$5d^7(^4P)6s\ ^3P_2$ - 6520^o_1	2161.1	0.0592	-5.622
$5d^66s^2\ ^5D_4$ - 6548^o_3	2163.7	0.0599	-5.618
$5d^66s^2\ ^5D_4$ - 6516^o_5	2178.5	0.0602	-5.622
$5d^7(^4F)6s\ ^5F_3$ - $5d^66s(^6D_{7/2})6p$ (7/2,1/2)$^o_3$	2179.0	0.0420	-5.778
$5d^7(^4P)6s\ ^5P_2$ - 6147^o_3	2182.8	0.0535	-5.675
$5d^7(^4P)6s\ ^3P_2$ - 6454^o_3	2192.5	0.0598	-5.630
$5d^8\ ^1G_4$ - 6273^o_4	2196.0	0.0103	-6.394
$5d^7(^4F)6s\ ^5F_4$ - $5d^66s(^6D_{9/2})6p$ (9/2,1/2)$^o_4$	2196.4	0.0381	-5.828
$5d^7(^4F)6s\ ^5F_3$ - $5d^7(^4F_{3/2})6p$ (3/2,1/2)$^o_2$	2197.5	0.0423	-5.782
$5d^7(^4P)6s\ ^3P_1$ - 6580^o_2	2203.7	0.0632	-5.611

Table 1. Continued

Transition	λ(Å)	FWHM(Å)	logW
$5d^7(^4F)6s\ ^5F_3$ - $5d^7(^4F_{7/2})6p\ (7/2,1/2)^o_4$	2204.9	0.0425	-5.784
$5d^7(^4F)6s\ ^5F_2$ - 5664^o_2	2205.0	0.0468	-5.741
$5d^7(^4P)6s\ ^3P_2$ - 6420^o_3	2208.6	0.0602	-5.634
$5d^66s^2\ ^5D_4$ - 6454^o_3	2208.7	0.0609	-5.629
$5d^7(^2G)6s\ ^3G_5$ - 6273^o_4	2209.0	0.0573	-5.655
$5d^7(^4F)6s\ ^3F_3$ - 6273^o_4	2210.0	0.0574	-5.655
$5d^7(^2G)6s\ ^3G_4$ - 6548^o_3	2212.3	0.0631	-5.615
$5d^8\ ^1D_2$ - $5d^66s(^6D_{7/2})6p\ (7/2,1/2)^o_3$	2217.1	0.0437	-5.776
$5d^7(^4P)6s\ ^5P_1$ - 6376^o_2	2217.2	0.0598	-5.640
$5d^7(^4F)6s\ ^5F_2$ - $5d^66s(^6D_{5/2})6p\ (5/2,1/2)^o_2$	2219.2	0.0471	-5.744
$5d^7(^4F)6s\ ^5F_3$ - $5d^7(^4P_{5/2})6p\ (5/2,1/2)^o_3$	2221.1	0.0428	-5.787
$5d^7(^4F)6s\ ^5F_2$ - $5d^7(^4P_{3/2})6p\ (3/2,1/2)^o_1$	2224.8	0.0472	-5.745
$5d^66s^2\ ^5D_4$ - 6420^o_3	2225.0	0.0612	-5.633
$5d^7(^2G)6s\ ^3G_4$ - 6516^o_5	2227.8	0.0634	-5.618
$5d^7(^4P)6s\ ^3P_2$ - 6376^o_2	2230.4	0.0607	-5.639
$5d^7(^4P)6s\ ^5P_2$ - 6046^o_2	2232.3	0.0545	-5.686
$5d^7(^4P)6s\ ^3P_1$ - 6520^o_1	2233.4	0.0639	-5.618
$5d^8\ ^1G_4$ - 6197^o_5	2233.4	0.0095	-6.443
$5d^8\ ^3F_4$ - $5d^7(^4F_{9/2})6p\ (9/2,1/2)^o_5$	2234.4	0.0358	-5.869
$5d^8\ ^1D_2$ - $5d^7(^4F_{3/2})6p\ (3/2,1/2)^o_2$	2236.3	0.0441	-5.780
$5d^7(^4P)6s\ ^5P_2$ - $5d^7(^4P_{1/2})6p\ (1/2,1/2)^o_1$	2236.6	0.0546	-5.687
$5d^7(^4F)6s\ ^5F_1$ - 5664^o_2	2237.1	0.0485	-5.739
$5d^7(^4P)6s\ ^5P_2$ - $5d^7(^4F_{9/2})6p\ (9/2,3/2)^o_3$	2239.6	0.0547	-5.688
$5d^8\ ^3P_1$ - $5d^7(^4F_{3/2})6p\ (3/2,1/2)^o_2$	2240.6	0.0443	-5.779
$5d^7(^4F)6s\ ^5F_5$ - $5d^7(^4F_{9/2})6p\ (9/2,1/2)^o_4$	2242.7	0.0336	-5.900
$5d^7(^4F)6s\ ^5F_2$ - $5d^7(^4F_{5/2})6p\ (5/2,1/2)^o_3$	2244.2	0.0476	-5.749
$5d^7(^4F)6s\ ^3F_4$ - $5d^7(^4F_{9/2})6p\ (9/2,3/2)^o_4$	2245.7	0.0483	-5.744
$5d^7(^2G)6s\ ^3G_5$ - 6197^o_5	2246.9	0.0582	-5.664
$5d^7(^4F)6s\ ^3F_2$ - 6690^o_3	2249.5	0.0688	-5.591
$5d^7(^4F)6s\ ^5F_1$ - $5d^66s(^6D_{5/2})6p\ (5/2,1/2)^o_2$	2251.7	0.0488	-5.742
$5d^7(^4F)6s\ ^5F_3$ - $5d^7(^4F_{5/2})6p\ (5/2,1/2)^o_2$	2255.5	0.0434	-5.794
$5d^7(^4F)6s\ ^5F_1$ - $5d^7(^4P_{3/2})6p\ (3/2,1/2)^o_1$	2257.5	0.0489	-5.743
$5d^8\ ^1G_4$ - 6148^o_4	2257.7	0.0090	-6.476
$5d^8\ ^1G_4$ - 6147^o_3	2258.5	0.0090	-6.478
$5d^7(^2G)6s\ ^3G_4$ - 6454^o_3	2259.4	0.0642	-5.626
$5d^8\ ^1D_2$ - $5d^7(^4P_{5/2})6p\ (5/2,1/2)^o_3$	2260.7	0.0446	-5.785
$5d^7(^4F)6s\ ^3F_4$ - $5d^7(^4F_{5/2})6p\ (5/2,1/2)^o_3$	2265.2	0.0486	-5.748
$5d^8\ ^3F_2$ - 6147^o_3	2268.9	0.0091	-6.477
$5d^7(^2G)6s\ ^3G_5$ - 6148^o_4	2271.4	0.0587	-5.669
$5d^7(^4F)6s\ ^3F_3$ - 6148^o_4	2272.5	0.0588	-5.669
$5d^7(^4F)6s\ ^3F_3$ - 6147^o_3	2273.3	0.0588	-5.669
$5d^7(^4P)6s\ ^5P_3$ - 5664^o_2	2275.7	0.0504	-5.737
$5d^7(^2G)6s\ ^3G_4$ - 6420^o_3	2276.5	0.0646	-5.629
$5d^8\ ^3F_3$ - $5d^7(^4F_{3/2})6p\ (3/2,1/2)^o_2$	2285.0	0.0464	-5.776
$5d^7(^2G)6s\ ^3G_3$ - 6690^o_3	2286.9	0.0715	-5.589

Table 1. Continued

Transition	λ(Å)	FWHM(Å)	logW
$5d^7(^4P)6s\ ^5P_3$ - $5d^6(^6D_{5/2})6p\ (5/2,1/2)^o_2$	2290.8	0.0508	-5.740
$5d^8\ ^3F_3$ - $5d^7(^4F_{7/2})6p\ (7/2,1/2)^o_4$	2293.0	0.0465	-5.778
$5d^8\ ^1D_2$ - $5d^7(^4F_{5/2})6p\ (5/2,1/2)^o_2$	2296.3	0.0452	-5.791
$5d^7(^4P)6s\ ^5P_3$ - $5d^7(^4F_{9/2})6p\ (9/2,3/2)^o_4$	2297.1	0.0509	-5.741
$5d^8\ ^3P_1$ - $5d^7(^4F_{5/2})6p\ (5/2,1/2)^o_2$	2300.9	0.0455	-5.791
$5d^7(^4F)6s\ ^3F_2$ - 6580^o_2	2306.8	0.0703	-5.604
$5d^7(^4P)6s\ ^3P_1$ - 6376^o_2	2307.4	0.0657	-5.634
$5d^7(^4F)6s\ ^5F_3$ - $5d^7(^4P_{5/2})6p\ (5/2,1/2)^o_2$	2314.9	0.0445	-5.805
$5d^7(^4P)6s\ ^5P_3$ - $5d^7(^4F_{5/2})6p\ (5/2,1/2)^o_3$	2317.4	0.0513	-5.745
$5d^8\ ^3F_2$ - 6046^o_2	2322.3	0.0080	-6.554
$5d^7(^4F)6s\ ^5F_3$ - $5d^7(^4F_{7/2})6p\ (7/2,1/2)^o_3$	2322.7	0.0447	-5.807
$5d^7(^4F)6s\ ^3F_2$ - 6548^o_3	2324.1	0.0707	-5.608
$5d^8\ ^1D_2$ - $5d^7(^4F_{3/2})6p\ (3/2,1/2)^o_1$	2324.7	0.0458	-5.797
$5d^7(^4F)6s\ ^3F_3$ - 6046^o_2	2327.0	0.0600	-5.680
$5d^8\ ^3P_1$ - $5d^7(^4F_{3/2})6p\ (3/2,1/2)^o_1$	2329.4	0.0460	-5.796
$5d^7(^4F)6s\ ^3F_3$ - $5d^7(^4F_{9/2})6p\ (9/2,3/2)^o_3$	2334.9	0.0602	-5.682
$5d^7(^4F)6s\ ^5F_2$ - $5d^6(^6D_{7/2})6s6p\ (7/2,1/2)^o_3$	2338.0	0.0495	-5.768
$5d^7(^4F)6s\ ^3F_2$ - 6520^o_1	2339.3	0.0711	-5.611
$5d^6(^5D_4)6s^2\ ^5D_4$ - 6197^o_5	2341.7	0.0640	-5.658
$5d^7(^4P)6s\ ^5P_2$ - $5d^6(^6D_{3/2})6s6p\ (3/2,1/2)^o_1$	2346.1	0.0571	-5.709
$5d^7(^2G)6s\ ^3G_3$ - 6580^o_2	2346.1	0.0571	-5.709
$5d^7(^4P)6s\ ^3P_2$ - 6147^o_3	2350.6	0.0635	-5.664
$5d^7(^2G)6s\ ^3G_4$ - 6273^o_4	2355.6	0.0666	-5.646
$5d^8\ ^1D_2$ - $5d^7(^4P_{5/2})6p\ (5/2,1/2)^o_2$	2357.9	0.0465	-5.803
$5d^7(^4F)6s\ ^5F_2$ - $5d^7(^4F_{3/2})6p\ (3/2,1/2)^o_2$	2359.4	0.0500	-5.772
$5d^7(^4F)6s\ ^3F_4$ - $5d^6(^6D_{7/2})6s6p\ (7/2,1/2)^o_3$	2360.7	0.0507	-5.766
$5d^8\ ^3F_4$ - $5d^7(^4F_{9/2})6p\ (9/2,1/2)^o_4$	2362.6	0.0380	-5.892
$5d^8\ ^3P_1$ - $5d^7(^4P_{5/2})6p\ (5/2,1/2)^o_2$	2362.8	0.0467	-5.802
$5d^8\ ^1D_2$ - $5d^7(^4F_{7/2})6p\ (7/2,1/2)^o_3$	2366.1	0.0467	-5.804
$5d^7(^4F)6s\ ^5F_4$ - $5d^7(^4F_{9/2})6p\ (9/2,1/2)^o_5$	2368.0	0.0411	-5.860
$5d^6(^5D_4)6s^2\ ^5D_4$ - 6148^o_4	2368.3	0.0647	-5.663
$5d^6(^5D_4)6s^2\ ^5D_4$ - 6147^o_3	2369.2	0.0647	-5.663
$5d^6(^5D_3)6s^2\ ^5D_3$ - 6580^o_2	2375.8	0.0752	-5.600
$5d^7(^4F)6s\ ^3F_4$ - $5d^7(^4F_{9/2})6p\ (9/2,3/2)^o_5$	2381.8	0.0511	-5.770
$5d^7(^4F)6s\ ^5F_2$ - $5d^7(^4P_{5/2})6p\ (5/2,1/2)^o_3$	2386.6	0.0506	-5.776
$5d^7(^4P)6s\ ^5P_1$ - $5d^6(^6D_{1/2})6s6p\ (1/2,1/2)^o_0$	2389.6	0.0640	-5.676
$5d^7(^4F)6s\ ^3F_4$ - $5d^7(^4F_{7/2})6p\ (7/2,1/2)^o_4$	2391.3	0.0513	-5.772
$5d^7(^4P)6s\ ^5P_1$ - 6046^o_2	2392.6	0.0641	-5.676
$5d^7(^2H)6s\ ^3H_5$ - 6678^o_5	2393.1	0.0791	-5.585
$5d^6(^5D_3)6s^2\ ^5D_3$ - 6548^o_3	2394.2	0.0758	-5.604
$5d^7(^4F)6s\ ^3F_2$ - 6420^o_3	2395.0	0.0726	-5.622
$5d^7(^4F)6s\ ^5F_1$ - $5d^7(^4F_{3/2})6p\ (3/2,1/2)^o_2$	2396.2	0.0518	-5.769
$5d^8\ ^3F_2$ - $5d^7(^4P_{3/2})6p\ (3/2,1/2)^o_2$	2396.2	0.0065	-6.673
$5d^7(^2G)6s\ ^3G_4$ - 6197^o_5	2398.7	0.0677	-5.654
$5d^7(^4F)6s\ ^3F_3$ - $5d^7(^4P_{3/2})6p\ (3/2,1/2)^o_2$	2401.2	0.0619	-5.694

Table 1. Continued

Transition	λ(Å)	FWHM(Å)	logW
$5d^7(^2F)6s\ ^3F_3$ - 7311^o_4	2403.6	0.0998	-5.488
$5d^7(^2H)6s\ ^3H_5$ - 6654^o_6	2407.0	0.0795	-5.588
$5d^7(^4F)6s\ ^3F_4$ - $5d^7(^4P_{5/2})6p$ (5/2,1/2)$^o_3$	2410.2	0.0518	-5.775
$5d^7(^4P)6s\ ^3P_2$ - $5d^7(^4P_{1/2})6p$ (1/2,1/2)$^o_1$	2413.1	0.0652	-5.676
$5d^7(^4P)6s\ ^3P_2$ - $5d^7(^4F_{9/2})6p$ (9/2,3/2)$^o_3$	2416.6	0.0653	-5.677
$5d^7(^4P)6s\ ^5P_3$ - $5d^6 6s(^6D_{7/2})6p$ (7/2,1/2)$^o_3$	2417.6	0.0536	-5.763
$5d^6 6s^2\ ^5D_2$ - 6690^o_3	2417.9	0.0814	-5.581
$5d^7(^4F)6s\ ^5F_2$ - $5d^7(^4F_{5/2})6p$ (5/2,1/2)$^o_2$	2426.3	0.0515	-5.783
$5d^7(^2G)6s\ ^3G_4$ - 6148^o_4	2426.7	0.0685	-5.660
$5d^7(^2G)6s\ ^3G_4$ - 6147^o_3	2427.6	0.0685	-5.660
$5d^6 6s^2\ ^5D_4$ - $5d^7(^4F_{9/2})6p$ (9/2,3/2)$^o_3$	2436.2	0.0665	-5.676
$5d^7(^4P)6s\ ^5P_2$ - 5664^o_2	2440.2	0.0594	-5.726
$5d^8\ ^3F_2$ - $5d^6 6s(^6D_{3/2})6p$ (3/2,1/2)$^o_1$	2445.8	0.0055	-6.765
$5d^7(^4P)6s\ ^5P_3$ - $5d^7(^4F_{7/2})6p$ (7/2,1/2)$^o_4$	2449.6	0.0543	-5.768
$5d^8\ ^3P_0$ - $5d^7(^4F_{3/2})6p$ (3/2,1/2)$^o_1$	2452.3	0.0519	-5.789
$5d^7(^4P)6s\ ^5P_2$ - $5d^6 6s(^6D_{5/2})6p$ (5/2,1/2)$^o_2$	2457.6	0.0598	-5.729
$5d^7(^4F)6s\ ^5F_2$ - $5d^7(^4F_{3/2})6p$ (3/2,1/2)$^o_1$	2458.0	0.0522	-5.788
$5d^7(^4P)6s\ ^5P_2$ - $5d^7(^4P_{3/2})6p$ (3/2,1/2)$^o_1$	2464.4	0.0600	-5.730
$5d^7(^4F)6s\ ^5F_1$ - $5d^7(^4F_{5/2})6p$ (5/2,1/2)$^o_2$	2465.2	0.0534	-5.781
$5d^7(^2D2)6s\ ^3D_3$ - 6690^o_3	2467.3	0.0853	-5.579
$5d^7(^4P)6s\ ^5P_3$ - $5d^7(^4P_{5/2})6p$ (5/2,1/2)$^o_3$	2469.5	0.0548	-5.771
$5d^8\ ^3F_3$ - $5d^6 6s(^6D_{9/2})6p$ (9/2,1/2)$^o_4$	2476.1	0.0505	-5.810
$5d^6 6s^2\ ^5D_2$ - 6580^o_2	2484.2	0.0834	-5.594
$5d^7(^4P)6s\ ^3P_2$ - $5d^7(^4P_{3/2})6p$ (3/2,1/2)$^o_2$	2487.5	0.0672	-5.689
$5d^7(^4P)6s\ ^5P_2$ - $5d^7(^4F_{5/2})6p$ (5/2,1/2)$^o_3$	2488.3	0.0606	-5.734
$5d^7(^2H)6s\ ^3H_5$ - 6516^o_5	2489.5	0.0820	-5.603
$5d^7(^4P)6s\ ^3P_1$ - $5d^6 6s(^6D_{1/2})6p$ (1/2,1/2)$^o_0$	2494.8	0.0707	-5.669
$5d^7(^4F)6s\ ^5F_2$ - $5d^7(^4P_{5/2})6p$ (5/2,1/2)$^o_2$	2495.2	0.0531	-5.794
$5d^6 6s^2\ ^5D_3$ - 6376^o_2	2496.9	0.0788	-5.623
$5d^7(^4F)6s\ ^5F_1$ - $5d^7(^4F_{3/2})6p$ (3/2,1/2)$^o_1$	2498.0	0.0542	-5.786
$5d^7(^4P)6s\ ^3P_1$ - 6046^o_2	2498.0	0.0708	-5.670
$5d^7(^2G)6s\ ^3G_4$ - $5d^7(^4F_{9/2})6p$ (9/2,3/2)$^o_3$	2498.0	0.0705	-5.672
$5d^6 6s^2\ ^5D_2$ - 6548^o_3	2504.4	0.0841	-5.598
$5d^7(^4P)6s\ ^5P_3$ - $5d^7(^4F_{5/2})6p$ (5/2,1/2)$^o_2$	2512.1	0.0558	-5.778
$5d^7(^4F)6s\ ^5F_4$ - $5d^7(^4F_{9/2})6p$ (9/2,1/2)$^o_4$	2512.6	0.0440	-5.882
$5d^7(^2H)6s\ ^3H_6$ - 6197^o_5	2517.9	0.0758	-5.648
$5d^7(^4F)6s\ ^3F_4$ - $5d^6 6s(^6D_{9/2})6p$ (9/2,1/2)$^o_5$	2523.6	0.0544	-5.793
$5d^7(^4P)6s\ ^5P_1$ - $5d^6 6s(^6D_{3/2})6p$ (3/2,1/2)$^o_1$	2523.9	0.0676	-5.699
$5d^7(^2G)6s\ ^3G_3$ - 6273^o_4	2528.4	0.0785	-5.636
$5d^7(^4F)6s\ ^3F_4$ - $5d^7(^4F_{7/2})6p$ (7/2,1/2)$^o_3$	2530.4	0.0546	-5.794
$5d^7(^2D2)6s\ ^3D_3$ - 6580^o_2	2536.4	0.0875	-5.591
$5d^7(^4F)6s\ ^5F_1$ - $5d^7(^4P_{5/2})6p$ (5/2,1/2)$^o_2$	2536.4	0.0551	-5.792
$5d^8\ ^3F_2$ - 5664^o_2	2548.2	0.0033	-7.015
$5d^7(^4F)6s\ ^3F_3$ - 5664^o_2	2553.8	0.0660	-5.720
$5d^7(^2D2)6s\ ^3D_3$ - 6548^o_3	2557.4	0.0883	-5.595

Table 1. Continued

Transition	λ(Å)	FWHM(Å)	logW
$5d^8\ {}^1G_4$ - $5d^7(^4F_{9/2})6p\ (9/2,3/2)^o_4$	2561.8	0.0027	-7.105
$5d^7(^4F)6s\ {}^3F_2$ - 6147^o_3	2562.9	0.0777	-5.652
$5d^7(^4F)6s\ {}^3F_3$ - $5d^66s(^6D_{5/2})6p\ (5/2,1/2)^o_2$	2572.9	0.0665	-5.723
$5d^8\ {}^3F_2$ - $5d^7(^4P_{3/2})6p\ (3/2,1/2)^o_1$	2574.7	0.0028	-7.102
$5d^7(^2G)6s\ {}^3G_5$ - $5d^7(^4F_{9/2})6p\ (9/2,3/2)^o_4$	2579.5	0.0667	-5.724
$5d^7(^4F)6s\ {}^3F_3$ - $5d^7(^4F_{9/2})6p\ (9/2,3/2)^o_4$	2580.9	0.0668	-5.724
$5d^7(^4P)6s\ {}^3P_1$ - $5d^7(^4P_{3/2})6p\ (3/2,1/2)^o_2$	2583.7	0.0734	-5.684
$5d^7(^4P)6s\ {}^5P_3$ - $5d^7(^4P_{5/2})6p\ (5/2,1/2)^o_2$	2586.1	0.0577	-5.789
$5d^8\ {}^1G_4$ - $5d^7(^4F_{5/2})6p\ (5/2,1/2)^o_3$	2587.1	0.0022	-7.206
$5d^7(^4F)6s\ {}^3F_4$ - $5d^66s(^6D_{9/2})6p\ (9/2,1/2)^o_4$	2591.0	0.0561	-5.803
$5d^7(^4P)6s\ {}^5P_3$ - $5d^7(^4F_{7/2})6p\ (7/2,1/2)^o_3$	2595.8	0.0580	-5.790
$5d^8\ {}^3F_2$ - $5d^7(^4F_{5/2})6p\ (5/2,1/2)^o_3$	2600.7	0.0022	-7.205
$5d^7(^4P)6s\ {}^5P_2$ - $5d^66s(^6D_{7/2})6p\ (7/2,1/2)^o_3$	2604.1	0.0637	-5.752
$5d^7(^4F)6s\ {}^3F_3$ - $5d^7(^4F_{5/2})6p\ (5/2,1/2)^o_3$	2606.6	0.0675	-5.728
$5d^7(^2G)6s\ {}^3G_3$ - 6148^o_4	2610.5	0.0811	-5.649
$5d^7(^4P)6s\ {}^5P_1$ - $5d^7(^4P_{1/2})6p\ (1/2,1/2)^o_0$	2617.1	0.0704	-5.713
$5d^7(^4P)6s\ {}^5P_1$ - 5664^o_2	2633.0	0.0709	-5.715
$5d^7(^4P)6s\ {}^3P_1$ - $5d^66s(^6D_{3/2})6p\ (3/2,1/2)^o_1$	2641.5	0.0752	-5.692
$5d^7(^4F)6s\ {}^3F_2$ - $5d^7(^4F_{9/2})6p\ (9/2,3/2)^o_3$	2641.5	0.0802	-5.664
$5d^7(^2H)6s\ {}^3H_5$ - 6273^o_4	2650.1	0.0875	-5.630
$5d^7(^4P)6s\ {}^3P_2$ - 5664^o_2	2651.8	0.0720	-5.714
$5d^7(^4P)6s\ {}^5P_1$ - $5d^66s(^6D_{5/2})6p\ (5/2,1/2)^o_2$	2653.3	0.0715	-5.718
$5d^7(^4P)6s\ {}^5P_3$ - $5d^66s(^6D_{9/2})6p\ (9/2,1/2)^o_4$	2659.7	0.0596	-5.799
$5d^7(^4P)6s\ {}^5P_1$ - $5d^7(^4P_{3/2})6p\ (3/2,1/2)^o_1$	2661.3	0.0717	-5.719
$5d^7(^4P)6s\ {}^5P_2$ - $5d^7(^4P_{5/2})6p\ (5/2,1/2)^o_3$	2664.5	0.0654	-5.760
$5d^7(^4P)6s\ {}^3P_2$ - $5d^7(^4P_{3/2})6p\ (3/2,1/2)^o_1$	2680.4	0.0729	-5.718
$5d^7(^2G)6s\ {}^3G_3$ - 6046^o_2	2682.7	0.0836	-5.660
$5d^7(^2G)6s\ {}^3G_3$ - $5d^7(^4F_{9/2})6p\ (9/2,3/2)^o_3$	2693.3	0.0839	-5.662
$5d^7(^2H)6s\ {}^3H_5$ - 6197^o_5	2704.9	0.0895	-5.638
$5d^66s^2\ {}^5D_4$ - $5d^7(^4F_{9/2})6p\ (9/2,3/2)^o_4$	2705.2	0.0745	-5.717

In [9], it is reported several lines of singly ionized iridium in the spectrum of χ Lupi. Many of them are blended so therefore there are difficulties to isolate one of them. In the case of iridium only one reasonably unblended line of Ir II was identified 2152.7 Å . In this contribution to the study of χ Lupi they used new accurate wavelengths and oscillator strengths from laboratory experiments for select lines of Os II and Ir II. In Fig. 1, we have shown the dependence for the Stark widths of temperatures calculated by the MSE method. We chosen two strongest lines from Ir II spectra: 2152.7 Å with relative intensity 8700 and very close 2242.7 Å with relative intensity 8000. One can see, as the temperature increases, the value for the Stark widths decreases, as usual. This is due to the line width formula [12] that depends reciprocally on the root temperature.

We have synthesized the line profiles of 21 Ir II strongest lines using SYNTH code [23] and the ATLAS9 code for stellar atmosphere models [24, 25] in the temperature range of 6000 $\leq T_{eff} \leq$ 16,000 K, and 4.0 $\leq$ log $g \leq$ 5.0. For calculations with SYNTH code we need logarithmic values of Stark widths expressed in $rads^{-1}$ per electron for T = 10,000 K. Also, for the spectrum synthesis parameter A_0 is very useful and can be obtained from corresponding values of log (A_0). In the case of 2152.7 Å we used log A_0=-0.49986 where A_0=4.81915.

We have analyzed the influence of electron-impact broadening mechanism on width ratio for 21 Ir II strongest lines. In our spectrum synthesis we used Solar value for iridium abundance -10.69. This is a much smaller value than represent in [9], but it is usefull for all stellar atmospheres where the presence of iridium varies between these values. In Fig. 2. we can notice for Ir II 2152.7 Å that the ratio of Stark and Doppler width increases with increasing temperature. The rate of change for widths is highest in the stellar atmospheres with an effective temperature of 6000 Kelvins. In this case we used generally for all lines parameter values for surface gravity log g=4 and turbulent velocity v_{turb}=2km/s. For this considered line, Stark broadening is more dominant than Doppler ones in all cases when the ratio of changes is greater than 1.

We have extended our analyzes of the strongest Ir II lines to test the dependence on the optical depth of the stellar atmosphere. One can see from Fig. 3. width ratio can be higher in the stars with high value of surface gravity. Especially for log g=5 we notice a higher slope of the curve and Stark broadening becomes more important than Doppler ones from -1 for the optical depth and it also points to deeper layers. As one can see from solid line and log g=4 Stark broadening is more important in photospheric layers. In our model we used T_{eff}=10000K and turbulent velocity v_{turb}=2km/s. Finally, in Fig. 4 we see an almost linear dependence of the width ratio as a function of temperature when we have a variable turbulent velocity in the stellar model. Here the functional dependences are approximately the same so the differences are very small regardless of the value of the turbulent velocity. Stark broadening becomes more significant at higher temperatures in atmospheres where the temperature is above 25,000 Kelvins. In this model we took T_{eff}=10000K and log g=4. For both Figs. 3 and 4 we can marked the point 1 on Y-axes, where above this point Stark broadening becomes more important tnan Doppler ones.

The experimental observation of the spectra of χ Lupi presented in [9] is used in order to check the validity of the theoretically calculated data. The fitting procedure is not related to any synthetic solar spectra model, and presents a best effort fit of the observed spectra to estimate the Stark parameters of Ir II 2282.279. Since the fine structure of the line is not considered, in order to distinguish a Lorentzian and Gaussian component the Voigt profile is used for the fitting of the line. The fitted parameters of the Voigth profile for the Ir II 2282.279 Å line are 0.0134 for the Lorentzian and 0.0368 for the Gauss component of the profile. This result lies in the vicinity of the expected, theoretically calculated values for the Lorentzian component and for the Gausian component of the line, see Fig. 5.

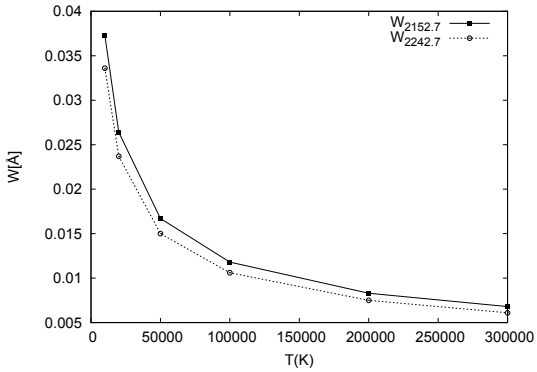

Fig. 1. Stark widths as a function of temperatures for singly ionized iridium spectral lines 2152.7 Å and 2242.7 Å spectral lines.

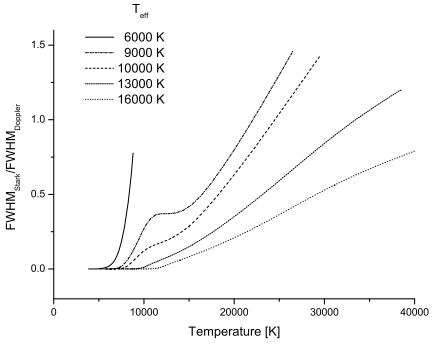

Fig. 2. Width ratio as a function of effective temperature, FWHM$_{Stark}$ - Stark width and FWHM$_{Doppler}$ - Doppler width, for the Ir II 2152.7 Å spectral line.

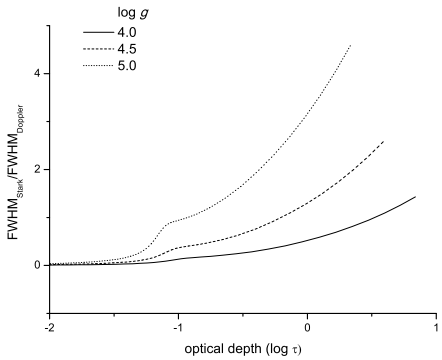

Fig. 3. Width ratio as a function of optical depth, FWHM$_{Stark}$ - Stark width and FWHM$_{Doppler}$ - Doppler width, for the Ir II 2152.7 Å spectral line.

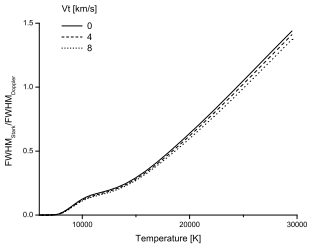

Fig. 4. Width ratio as a function of effective temperature, FWHM$_{Stark}$ - Stark width and FWHM$_{Doppler}$ - Doppler width, for the Ir II 2152.7 Å spectral line.

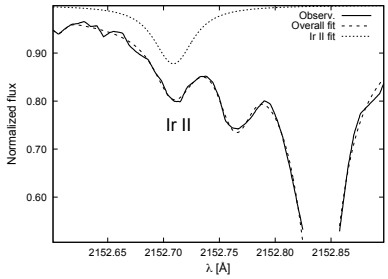

Fig. 5. From the observed spectrum of χ Lupi presented in [9], the fitting procedure is used to extracted the Ir II 2152.7 Å line parameters assuming the Voigt line profile. The solid line presents experimental observation spectra, while the long dashed line is the overall fit, and short dash line is the sought line fit.

4 CONCLUSION

The development of satellite spectroscopy has made available spectra of stars containing heavy elements and elements from the group of rare earths. In this paper, attention is focused to single ionized iridium, which is detected in the atmospheres of hot stars, χ Lupi, so - called CP stars. This element whose energy levels have been determined for 301 known lines in the previous decade relatively recently. For calulation we chosen MSE method to obtain Stark widths of this singly ionezed iridium. In our analysis we took a total of 21 strongest lines from the singly ionized iridium spectrum and whose intensities exceed the value of 3000. The Stark broadening mechanism is very important for A and B type of stellar atmospheres as well as for white dwarfs atmospheres, and one has to take into account this effect for investigations, analysis and modeling of such stellar atmospheres. In terms of determining the equivalent width, the errors range between 10 % up to 45 %, so they are appropriate errors in determining abundance are similar.

The total number of 301 spectral lines of Ir II presented here is an extensive task, so we plan to continue research on another 172 lines from its spectrum whose intensities are much lower. This paper contributes to the formation of a database on the Stark broadening of ionized iridium spectral lines.

These calculations are useful for spectroscopy in further even more precise determination of the representation of heavy elements in stellar spectra as well as in laboratory and technological plasma.

ACKNOWLEDGEMENT

This work is supported by Ministry of Education, Science and Technological Development of the Republic of Serbia through the project contract No. 451-03-68/2020/14/200002.

COMPETING INTERESTS

Authors have declared that no competing interests exist.

REFERENCES

[1] Leckrone David S, Proffitt Charles R, Wahlgren Glenn M, Johansson Sveneric G, Brage Tomas. Very High Resolution Ultraviolet Spectroscopy of a Chemically Peculiar Star: Results of the chi LUPI Pathfinder Project. Astronomical Journal. 1999;117(3):1454-1470.

[2] Wyart JF, Raassen AJJ, Uylings PHM, Joshi YN. Spectra of high-Z ions of stellar interest. A theoretical study of $(d+s)^8$ mixed configurations in 5d- and 4d-elements. Physica Scripta Volume T. 1993;47:59-64.

[3] Popović L. Č, Dimitrijević MS, Ryabchikova T. The electron-impact broadening effect in CP stars: the case of La II , La II i, EU II , and EU II i lines. Astronomy and Astrophysics. 1999;350:719-724.

[4] Popović LČ, Simić S, Milovanović N, Dimitrijević MS. Stark Broadening Effect in Stellar Atmospheres: Nd II Lines. The Astrophysical Journal Supplement Series. 2001;135(1):109—114.

[5] Grevesse N, Sauval AJ. Standard Solar Composition. Space Science Reviewsc. 1998;85: 161-174.

[6] Grevesse N, Sauval AJ. Abundances of the Elements in the Sun. In O. Manuel editor, Origin of Elements in the Solar System, Implications of Post-1957 Observations. 2000;261.

[7] Xu HL, Svanberg S, Quinet P, Palmeri P, Biémont É. Improved atomic data for iridium atom (Ir I) and ion (Ir II) and the solar content of iridium. Journal of Quantitiative Spectroscopy and Radiative Transfer. 2007;104(1):52-70.

[8] Wahlgren Glenn M, Leckrone David S, Johansson Sveneric G, Rosberg Maria, Brage Tomas. The Abundances of Pt, Au, and HG in the Chemically Peculiar HgMn-Type Stars kappa CANCRI and chi LUPI. Astrophysical Journal, Supplement. 1995;444:438.

[9] Ivarsson S, Wahlgren GM, Dai Z, Lundberg H, Leckrone DS. Constraining the very heavy elemental abundance peak in the chemically peculiar star χ Lupi, with new atomic data for Os II and Ir II. Astronomy and Astrophysics. 2004;425:353-360.

[10] van Kleef Th. AM, Metsch BC. Term analysis of singly ionized iridium (Ir II). Physica B+C. 1978;95(2):251-265.

[11] Kramida AE. The program LOPT for least-squares optimization of energy levels. Computer Physics Communications. 2011;182(2):419-434.

[12] Dimitrijević MS, Konjević N. Stark widths of doubly- and triply-ionized atom lines. Journal of Quantitative Spectroscopy and Radiative Transfer. 1980;24(6):451-459.

[13] Griem Hans R. Semiempirical Formulas for the Electron-Impact Widths and Shifts of Isolated Ion Lines in Plasmas. Physical Review. 1968;165(1):258-266.

[14] Sahal-Bréchot S. Impact Theory of the Broadening and Shift of Spectral Lines due to Electrons and Ions in a Plasma. Astronomy and Astrophysics. 1969;1:91.

[15] Sahal-Bréchot S. Impact Theory of the Broadening and Shift of Spectral Lines due to Electrons and Ions in a Plasma (Continued). Astronomy and Astrophysics. 1969;2: 322.

[16] Dimitrijević MS, Konjević N. Simple estimates for Stark broadening of ion lines in stellar plasmas. Astronomy and Astrophysics. 1987;172(1-2):345-349.

[17] Bates DR, Agnete Damgaard. The Calculation of the Absolute Strengths of Spectral Lines. Philosophical Transactions of the Royal Society of London. Series

A, Mathematical and Physical Sciences. 1949;242(842):101-122.

[18] Shore Bruce W, Menzel Donald H. Generalized Tables for the Calculation of Dipole Transition Probabilities. Astrophysical Journal, Supplement. 1965;12:187.

[19] Cowley CR. An approximate Stark broadening formula for use in spectrum synthesis. The Observatory. 1971;91: 139-140.

[20] Popović L Č, Dimitrijević MS. Stark broadening of heavy ion lines: As II, Br II, Sb II and I II. Physica Scripta. 1996;53:325.

[21] Popović LČ, Dimitrijević MS. Stark broadening of Xe II lines. Astronomy and Astrophysics, Supplement. 1996; 116:359-365.

[22] Milovanović N, Dimitrijević MS, Popović LČ, Simić Z. Importance of collisions with charged particles for stellar UV line shapes: Cd III. Astronomy and Astrophysics. 2004;417:375-380.

[23] Piskunov NE. SYNTH - a code for rapid spectral synthesis. In Physics and Evolution of Stars: Stellar Magnetism. 1992;92.

[24] Kurucz Robert. Atomic Data for Ca, Sc, Ti, V, Cr, Mn, Co, Fe and Ni. Atomic Data for Ca, Sc, Ti, V, Cr, Mn, Co,Fe and Ni. Kurucz CD-ROM No. 20 - 22. Cambridge. 1994;20-22.

[25] Kurucz Robert. ATLAS9 Stellar Atmosphere Programs and 2 km/s grid. ATLAS9 Stellar Atmosphere Programs and 2 km/s grid. Kurucz CD-ROM No. 13. Cambridge. 1993;13.

Peer-review history:
The peer review history for this paper can be accessed here:
http://www.sdiarticle4.com/review-history/70329